RESEARCH

Open Access

Elevated CSF inflammatory markers in patients with idiopathic normal pressure hydrocephalus do not promote NKCC1 hyperactivity in rat choroid plexus

Sara Diana Lolansen[1], Nina Rostgaard[2], Søren Norge Andreassen[1], Anja Hviid Simonsen[3], Marianne Juhler[2], Steen Gregers Hasselbalch[3] and Nanna MacAulay[1*]

Abstract

Background: Idiopathic normal pressure hydrocephalus (iNPH) is a potentially reversible neurological condition of unresolved etiology characterized by a clinical triad of symptoms; gait disturbances, urinary incontinence, and cognitive deterioration. In the present study, we aimed to elucidate the molecular coupling between inflammatory markers and development of iNPH and determine whether inflammation-induced hyperactivity of the choroidal $Na^+/K^+/2Cl^-$ cotransporter (NKCC1) that is involved in cerebrospinal fluid (CSF) secretion could contribute to the iNPH pathogenesis.

Methods: Lumbar CSF samples from 20 iNPH patients (10 with clinical improvement upon CSF shunting, 10 without clinical improvement) and 20 elderly control subjects were analyzed with the novel proximity extension assay technique for presence of 92 different inflammatory markers. RNA-sequencing was employed to delineate choroidal abundance of the receptors for the inflammatory markers found elevated in the CSF from iNPH patients. The ability of the elevated inflammatory markers to modulate choroidal NKCC1 activity was determined by addition of combinations of rat version of these in ex vivo experiments on rat choroid plexus.

Results: 11 inflammatory markers were significantly elevated in the CSF from iNPH patients compared to elderly control subjects: CCL28, CCL23, CCL3, OPG, CXCL1, IL-18, IL-8, OSM, 4E-BP1, CXCL6, and Flt3L. One inflammatory marker, CDCP1, was significantly decreased in iNPH patients compared to control subjects. None of the inflammatory markers differed significantly when comparing iNPH patients with and without clinical improvement upon CSF shunting. All receptors for the elevated inflammatory markers were expressed in the rat and human choroid plexus, except CCR4 and CXCR1, which were absent from the rat choroid plexus. None of the elevated inflammatory markers found in the CSF from iNPH patients modulated the choroidal NKCC1 activity in ex vivo experiments on rat choroid plexus.

Conclusion: The CSF from iNPH patients contains elevated levels of a subset of inflammatory markers. Although the corresponding inflammatory receptors are, in general, expressed in the choroid plexus of rats and humans, their activation did not modulate the NKCC1-mediated fraction of choroidal CSF secretion ex vivo. The molecular mechanisms underlying ventriculomegaly in iNPH, and the possible connection to inflammation, therefore remains to be elucidated.

*Correspondence: macaulay@sund.ku.dk
[1] Department of Neuroscience, University of Copenhagen, Blegdamsvej 3B, 2200 Copenhagen, Denmark
Full list of author information is available at the end of the article

Lolansen *et al. Fluids and Barriers of the CNS*   (2021) 18:54

Page 2 of 15

Background

Idiopathic normal pressure hydrocephalus (iNPH) is a potentially reversible neurological condition first described by Hakim and Adams in 1965 [1]. INPH primarily affects adults above 65 years of age [2, 3] and the condition is characterized by a clinical triad of symptoms; gait disturbances, urinary incontinence, and cognitive deterioration [1, 4]. Patients with iNPH accumulate excessive amounts of cerebrospinal fluid (CSF) in their brain ventricles causing ventricular enlargement [4] and drainage by shunt insertion often improves the patient's clinical status [5–11]. Such direct reversibility of the clinical symptoms points to excessive CSF accumulation as part of the etiology, rather than permanent brain damage. The intracranial pressure (ICP) in iNPH patients is generally below 15 mmHg [9, 10, 12, 13] which is believed to resemble the ICP in healthy individuals [14, 15], hence the term *normal pressure* hydrocephalus. However, since reference ICP values in healthy individuals remain sparse and pseudo-healthy patients are often used instead [16] it is still debated whether the ICP in this patient group is truly resembling the ICP of healthy individuals. The etiology of iNPH remains unresolved but impaired CSF drainage or CSF hypersecretion may underlie the excessive CSF accumulation and possible ICP elevation. Although no macroscopic obstruction is discernible on diagnostic imaging [4, 17] some iNPH patients display elevated CSF outflow resistance [12, 18, 19] suggesting impaired CSF clearance and absorption. On the other hand, the CSF flow in iNPH patients appears hyperdynamic as demonstrated by an increased aqueductal CSF flow [20–24]. This hyperdynamic CSF flow may originate from a decreased intracranial compliance [13, 25–29] but could alternatively be explained by CSF hypersecretion, a potential mechanism generally neglected in the pathogenesis of hydrocephalus. CSF hypersecretion is sufficient to promote hydrocephalus development in humans [30–32] and animals [33] and has been demonstrated to occur in rats upon activation of an inflammatory pathway involving toll-like receptor 4 and NF$\kappa\beta$ in the CSF-producing tissue, the choroid plexus [33]. Altered abundance of select inflammatory markers has been detected in CSF from various hydrocephalic patients [34]. Elevated levels of inflammatory markers may potentially correlate with several factors affecting the prognosis; e.g. the risk of development of some forms of hydrocephalus, the severity of the condition, and the need for surgical intervention [35–38], while treatment with anti-inflammatory drugs reduces the incidence of hydrocephalus and improves clinical outcome [39, 40]. We hypothesize that inflammation-induced CSF hypersecretion may underlie the CSF accumulation seen in iNPH patients, in whom there is no visible CSF drainage obstruction and in whom the underlying pathological mechanism therefore remains unresolved. In the present study, we sought to elucidate the molecular coupling between inflammatory markers and development of iNPH by revealing the inflammatory marker profile in CSF from iNPH patients alongside the delineation of the abundance of the corresponding receptors in the choroid plexus. The connection between the inflammatory marker profile in this patient group and hyperactivity of the choroidal $Na^+/K^+/2Cl^-$ (NKCC1) transport mechanism, illustrated to sustain approximately 50% of the CSF secretion by the choroid plexus [33, 41, 42], was determined in an ex vivo rodent animal model. If inflammatory markers are involved in the pathogenesis of iNPH, pharmacological targeting of their receptors or downstream signaling pathways could prove a novel treatment strategy.

Methods

Study population

Lumbar CSF samples from 20 iNPH patients (mean age: 77 years, range: 71–83 years, 10 M/10 F) and 20 elderly control subjects of similar age and sex distribution (mean age: 67 years, range: 58–81 years, 11 M/9 F) were provided retrospectively by the Danish Dementia Biobank at the Danish Dementia Research Centre (Copenhagen University Hospital, Rigshospitalet, Denmark). The patients were diagnosed in accordance with the international iNPH guidelines [4]; ventricular enlargement on brain imaging, presence of clinical symptoms (gait/balance disturbance present, plus at least one other area of impairment in cognition, urinary symptoms, or both), and normal CSF opening pressure. Gait and incontinence was scored using validated clinical scales [43] and cognition was scored by MMSE [44]. Ten iNPH patients (mean age: 78 years, range: 71–83 years, 5 M/5 F) were classified as "responders" based on improvement of clinical symptoms after surgical insertion of a ventriculo-peritoneal (VP) shunt. The ten remaining iNPH patients (mean age: 76 years, range: 71–82 years, 5 M/5 F) were classified as "non-responders" based on lack of clinical improvement despite surgical intervention with the VP shunt. Response to VP shunt was evaluated 6 months post surgery by reevaluating the clinical symptoms using the clinical scales above. Inclusion criteria for the iNPH group were (1) sample availability from the biobank (2)

Lolansen *et al. Fluids and Barriers of the CNS*   (2021) 18:54

Page 3 of 15

shunt surgery was performed at the Department of Neurosurgery at Rigshospitalet and (3) follow-up data available on shunt response. All elderly control subjects were referred for diagnostic workup for cognitive impairment including neurological and cognitive examination, diagnostic lumbar puncture, and brain imaging. The clinical investigations did not show any signs of cognitive decline, abnormal CSF, or imaging biomarkers. Furthermore, the subjects did not fulfill the iNPH criteria [4], the criteria for dementia [45], or mild cognitive impairment [46] and were thus included as the elderly control group. Table 1 summarizes the clinical characteristics of the study population. Written informed consent was obtained from patients and control subjects. The study was approved by the Ethics committee of the Capital Region of Denmark.

Cerebrospinal fluid samples
CSF samples were obtained by lumbar puncture between 9 a.m. and 1 p.m. The first 4 ml were collected for routine investigations and the following 8–12 ml were collected in polypropylene tubes, centrifuged at $2000 \times g$ for 10 min, the supernatant was aliquoted into cryo tubes and stored at $- 80$ °C within two hours from sampling according to previous recommendations [47]. The CSF samples were thawed only once for aliquoting prior to analysis. The CSF samples from the iNPH patients were taken as part of the diagnostic workup for iNPH.

Proximity extension assay
BioXpedia A/S (Aarhus, Denmark) analyzed CSF samples for presence of 92 different inflammatory markers (Inflammation panel, Art. No. 95301) using the novel proximity extension assay (PEA) technique (Olink Bioscience, Sweden) [48]. In brief, the PEA technique employs a pair of oligonucleotide-conjugated antibodies to detect each inflammatory marker in a CSF volume of 1 µl. Upon detection, the oligonucleotides are brought in close proximity, hybridize, and enable DNA polymerization, which produces a PCR sequence. The PCR sequence is amplified and quantified using microfluidic real-time PCR. The PEA technique outputs relative protein values measured in normalized protein expression (NPX), and thus cannot provide the actual concentrations of the markers present in the CSF. The higher the protein abundance in the CSF sample, the higher the NPX value. In addition to the CSF samples, two plasma samples obtained from two randomly chosen elderly control subjects were analyzed for assay validation.

Experimental animals
All procedures involving experimental animals conformed to the legislations for animal protection and care provided in the European Community Council Directive (2010/63/EU) and complied with the ARRIVE guidelines [49]. Nine-week-old adult male Sprague Dawley rats (Janvier Labs) were used for all experiments. The animals had food and water available ad libitum and were housed with a 12:12 light cycle.

Choroid plexus isolation and culturing
Rats were anesthetized with an intraperitoneal injection of ketamine and xylazine (60 mg/ml, 6 mg/ml, 0.17 ml per 100 g body weight, ScanVet) and quickly decapitated. Isolated rat brains were immersed in ice-cold artificial CSF (aCSF) containing (in mM): 120 NaCl, 2.5 KCl, 2.5 $CaCl_2$, 1.3 $MgSO_4$, 1 NaH_2PO_4, 10 glucose, 17 Na-HEPES, pH 7.4. Rat brains were kept in ice-cold aCSF for 10 min followed by separation of the two hemispheres and isolation of the choroid plexus from the lateral ventricles. The acutely isolated lateral choroid plexus was placed in Dulbecco's Modified Eagle's Medium (DMEM1965, high glucose, $NaHCO_3{}^-$, HEPES, Gibco) supplemented with penicillin–streptomycin (100 U/ml, 100 µg/ml, Gibco), rat epidermal growth factor (10 ng/ml, SRP3238, Sigma), and fetal bovine serum (10%, 04-007-1A, Biological Industries) (DMEM growth medium). As inflammatory

Table 1 Clinical characteristics of the study population

Characteristics	All iNPH patients	iNPH responders	iNPH non-responders	Elderly control subjects
N	20	10	10	20
Age (mean, range)	77y, 71–83y	78y, 71–83y	76y, 71–82y	67y, 58–81y
Sex (M/F)	10/10	5/5	5/5	11/9
MMSE (mean, range)	25 (15–29)	24 (15–29)	26 (23–29)	29 (25–30)
Gait score	3 (1–5)	3 (2–4)	3 (1–5)	NA
Urinary continence score	3 (1–5)	3 (1–5)	3 (1–4)	NA

Gait score: 0—normal, 8—wheelchair bound, Urinary continence score: 0—normal, 6—bladder and bowel incontinence [43]

iNPH idiopathic normal pressure hydrocephalus

markers may exert their effect on cells and tissue on a longer time scale, the choroid plexus was incubated for 16 h at 37 °C, 5% CO_2 in presence of select inflammatory markers (or vehicle). To verify choroid plexus viability during the 16 h culturing ex vivo, we performed calcein acetoxymethyl (calcein-AM) staining and evaluated the tissue by microscopy [50]. Viable cells contain active intracellular esterases that cleave the AM group from the calcein, resulting in a bright fluorescent signal from these viable cells. After isolation from the lateral ventricles, the choroid plexus tissue was placed in DMEM growth medium and left for 16 h at 37 °C, 5% CO_2 prior to incubation in aCSF containing calcein-AM (16.7 μM) for 10 min at room temperature. An acutely isolated choroid plexus was employed as a positive control and the negative control consisted of an acutely isolated choroid plexus placed in distilled water (dH_2O) for 16 h prior to calcein-AM staining. Images were acquired using Zeiss Axioplan 2 microscope equipped with epifluorescence and interference filters with a 702 moni AxioCam, and using Zeiss Zen Black software.

Isotope efflux experiments
Following 16 h of incubation, the choroid plexus was allowed to recover for 10 min in 37 °C aCSF prior to 10 min of incubation in isotope solution containing: $^{86}Rb^+$ (1 μCi/ml, 022-105721-00321-0001, POLATOM) and ^3H-mannitol (4 μCi/ml, NET101, Perkin Elmer). ^3H-mannitol does not enter the choroid plexus and serves as an extracellular marker [51]. After isotope incubation, the choroid plexus was briefly rinsed in isotope-free aCSF followed by transfer into new wells containing isotope-free aCSF at regular intervals as indicated on the figure. For every time point, 0.2 ml of surrounding aCSF was collected and placed into scintillation vials. At the end of the experiment, the choroid plexus was placed into a scintillation vial containing 0.2 ml Solvable (6NE9100, Perkin Elmer) and dissolved at room temperature for a minimum of 4 h. The isotope content was determined in 2 ml Ultima Gold™ XR scintillation liquid (6013119, Perkin Elmer) using the Tri-Carb 2900TR Liquid Scintillation Analyzer (Packard). For each time point, the $^{86}Rb^+$ activity was corrected for extracellular background using ^3H-mannitol. Data are shown as the natural logarithm of the $^{86}Rb^+$ activity at time each point (A_T) normalized to the initial $^{86}Rb^+$ activity (A_0) as a function of time. The slope from linear regression analysis was used to determine the $^{86}Rb^+$ efflux rate constant (min^{-1}) in absence (including vehicle) and presence of bumetanide (B3023, Sigma; 20 μM made up from a stock solution of 20 mM in DMSO) or select inflammatory markers [41, 51].

RNA sequencing
STAR-RNA and RSEM parameter settings for the library build, mapping and quantification, together with all scripts for the gene annotation and analysis are available online at https://github.com/Sorennorge/MacAulayLab-RNAseq1 [52]. Rat choroid plexus (laterals and 4th) was isolated in ice-cold aCSF and stored in RNAlater (R0901, Sigma) at − 80 °C. The RNA extraction and library preparation were performed by Novogene Company Limited, UK with NEB Next® Ultra™ RNA Library Prep Kit (NEB, USA) prior to RNA sequencing (paired-end 150 bp, with 15 Gb output) on an Illumina NovaSeq 6000 (Illumina, USA). Novogene performed QC and removed low quality reads and adapters. The 150 base paired-end reads were mapped to Reference genome Rnor_6.0 (Rattus_norvegicus) using Spliced Transcripts Alignment to a Reference (STAR) RNA-seq aligner (v 2.7.2a) [53]. The mapped alignment generated by STAR was normalized to transcripts per million (TPM) [54] with RSEM (v. 1.3.3) [55]. Gene information was gathered with mygene (v 3.1.0) python library [56, 57], https://mygene.info [58]. The human choroid plexus data was publicly available and obtained from the Gene Expression Omnibus (GEO) database, accession number GSE137619 (SRR10134643-SRR10134648), https://www.ncbi.nlm.nih.gov/geo/query/acc.cgi?acc=GSE137619 [59]. The data were quality controlled with Fastqc (available online at http://www.bioinformatics.babraham.ac.uk/projects/fastqc [60]) and trimmed with Trimmomatic [61] (quality below 20, minimum length of 35 bp). The six human choroid plexus samples were mapped, with similar settings as the rat choroid plexus sample, to the reference genome GRCh38 (Homo sapiens) with STAR and quantified with RSEM, and the mean TPM of the six samples was used for the analysis.

Inflammatory markers for $^{86}Rb^+$ efflux experiments
Rat interleukin-18 (IL-18, cat. no. 521-RL-025) was purchased from R&D Systems (UK). Rat C–C motif chemokine ligand 28 (CCL28, cat. No. chm-278), rat CCL6 (cat. no. chm-268), rat CCL3 (cat. no. chm-343), and rat oncostatin-M (OSM, cat. no. cyt-169) were purchased from ProSpec (Israel). Rat C-X-C motif chemokine ligand 1 (CXCL1, Cat. No. SRP3240) was purchased from Sigma (USA). All chemicals were dissolved in sterile water or phosphate buffered saline supplemented with 0.1% bovine serum albumin (A6003, Sigma) to a stock concentration of 100 μg/ml and kept frozen in aliquots at − 20 °C until use to avoid repeated freeze–thaw cycles. Final concentrations are indicated in the Figure legends.

Statistics

Data analysis and statistical tests were conducted in GraphPad Prism version 8 (GraphPad Software). *Inflammatory markers in CSF:* The limit of detection (LOD) was calculated for each inflammatory marker as the background signal plus two times the standard deviation of the inflammatory marker. Inflammatory markers were excluded from further analysis if > 35% of the samples were below the LOD. This criterion led to the exclusion of 33 inflammatory markers. None of the excluded inflammatory markers showed any tendency towards preferential presence in one of the study groups. The remaining 59 inflammatory markers were included in the statistical analysis. Additional file 1: Table S1, provides an overview of the excluded and included inflammatory markers. For normally distributed data, an unpaired two-tailed T-test was conducted and a Welch's correction was applied if variances were unequal. For non-normally distributed data, a Mann–Whitney test was conducted. $P < 0.05$ was considered statistically significant. P-values were not corrected for multiple comparisons [62] as it was desired to identify as many potential candidates as possible for subsequent rodent functional experimentation, which would determine the pathophysiological role of the inflammatory markers on choroidal CSF secretion. Additional file 2: Table S2 and Additional file 3: Table S3, provide an overview of the statistical tests and results for each inflammatory marker. $^{86}Rb^+$ *efflux experiments:* Data are presented as mean ± standard deviation and n corresponds to the number of individual animals. Data were analyzed with an unpaired two-tailed t-test and $P < 0.05$ was considered statistically significant.

Results

Inflammatory markers are elevated in CSF from iNPH patients

To determine if iNPH patients displayed altered CSF distribution of inflammatory markers, we compared lumbar CSF from 20 iNPH patients and 20 elderly control subjects. The clinical characteristics of the study groups are summarized in Table 1. Quantification of 92 different inflammatory markers was obtained using the novel PEA technique, which relies on dual antibody-based recognition of each inflammatory marker, providing a high throughput with excellent specificity and sensitivity [48]. The CSF levels of 11 inflammatory markers were significantly elevated in iNPH patients compared to elderly control subjects: CCL28, CCL23, CCL3, osteoprotegerin (OPG), CXCL1, IL-18, IL-8, OSM, eukaryotic translation initiation factor 4E-binding protein 1 (4E-BP1), CXCL6, and fms-related tyrosine kinase 3 ligand (Flt3L) (Table 2). The majority of the elevated inflammatory markers were chemokines (CCL28, CCL23, CCL3, CXCL1, and CXCL6) or interleukins (IL-18 and IL-8), small secreted proteins that drive and modulate immune responses in a pleiotropic manner, depending on their target [63, 64].

The CSF level of one inflammatory marker, CUB domain-containing protein 1 (CDCP1), a transmembrane glycoprotein chemotactic for T-cells [65], was significantly decreased in iNPH patients compared to the group of elderly control subjects (iNPH: 4.576 ± 0.245 NPX; elderly control subjects: 4.905 ± 0.556 NPX, P = 0.0225).

INPH patients often improve clinically upon VP shunt insertion [5–11]. However, as some patients fail to improve, the underlying etiology may potentially differ, which could give rise to differences in the CSF

Table 2 Elevated inflammatory markers in CSF from iNPH patients

Inflammatory marker	Full name	iNPH patients	Elderly control subjects	Percent increase (%)	P-value
CCL28	C–C motif chemokine ligand 28	1.749 ± 0.222	1.495 ± 0.265	19	0.0007
CCL23	C–C motif chemokine ligand 23	3.260 ± 0.451	2.993 ± 1.013	20	0.0051
CCL3	C–C motif chemokine ligand 3	4.506 ± 0.433	4.262 ± 0.973	18	0.0056
OPG	Osteoprotegerin	10.150 ± 0.529	9.765 ± 0.478	31	0.0207
CXCL1	C-X-C motif chemokine ligand 1	6.646 ± 0.524	6.408 ± 1.091	18	0.0211
IL-18	Interleukin-18	2.639 ± 0.595	2.409 ± 1.093	17	0.0227
IL-8	Interleukin-8	8.497 ± 0.506	8.275 ± 0.787	17	0.0263
OSM	Oncostatin-M	0.726 ± 0.373	0.655 ± 0.915	5	0.0283
4E-BP1	Eukaryotic translation initiation factor 4E-binding protein 1	2.763 ± 0.653	2.544 ± 1.177	16	0.0283
CXCL6	C-X-C motif chemokine ligand 6	4.246 ± 0.637	3.929 ± 1.353	25	0.0375
Flt3L	Fms-related tyrosine kinase 3 ligand	9.100 ± 0.356	8.909 ± 0.515	14	0.0402

Data are expressed as normalized protein expression (NPX) values (mean ± SD), an arbitrary unit on $\log_2$ scale. Percent increase represents the increase in iNPH CSF compared to CSF from elderly control subjects. Data were analyzed with an unpaired two-tailed T-test or a Mann–Whitney test. iNPH = idiopathic normal pressure hydrocephalus

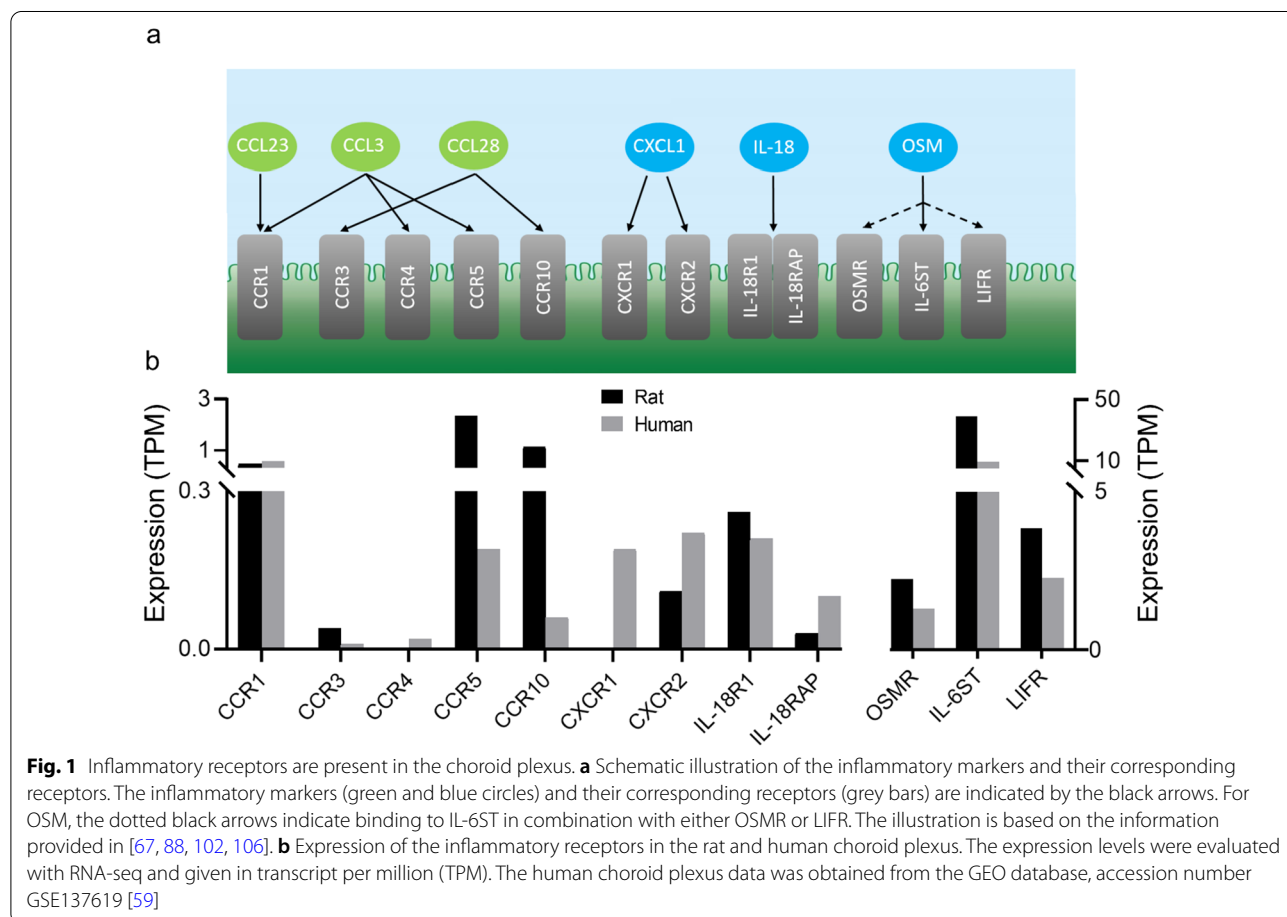Lolansen *et al. Fluids and Barriers of the CNS*   (2021) 18:54

Page 6 of 15

distribution of inflammatory markers. To determine if the inflammatory profile of iNPH patients with clinical improvement upon VP shunting (iNPH responders) differed from those who did not improve (iNPH non-responders), we compared the inflammatory CSF marker content of the two patient groups, but found none of the inflammatory markers to differ significantly (see Additional file 2: Table S2 and Additional file 3: Table S3, for all statistical tests). Taken together, our findings demonstrate that the molecular profile of the CSF from iNPH patients contains elevated levels of inflammatory markers and that the inflammatory marker profile of iNPH responders and iNPH non-responders is indistinguishable prior to VP shunt insertion.

Inflammatory receptors are present in the choroid plexus
Of the 11 inflammatory markers significantly elevated in the CSF from iNPH patients, eight were selected as candidates for further ex vivo investigation of their ability to modulate the transport activity in choroid plexus: CCL28, CCL23, CCL3, CXCL1, IL-18, IL-8, OSM and CXCL6. The remaining inflammatory markers OPG,

4E-BP1, and Flt3L were not investigated further as they serve physiological roles which make them less likely to directly influence choroidal CSF secretion.

The ability of the eight candidate inflammatory markers to alter choroidal transporter activity requires that their respective receptors are expressed in choroid plexus (Fig. 1a). Such verification was obtained by transcriptional analysis (RNA-seq) of the choroid plexus. The ex vivo determination of choroid plexus transport activity cannot be conducted in human choroid plexus. Therefore we employed rat choroid plexus for the functional assay described below and hence performed the RNA-seq on acutely isolated rat choroid plexus. RNA-seq revealed that the majority of the inflammatory receptors targeted by the detected inflammatory markers were expressed in the rat choroid plexus, albeit at variable levels (Fig. 1b). The inflammatory receptors C–C motif chemokine receptor 1 (CCR1), CCR3, C-X-C motif chemokine receptor 2 (CXCR2), IL-18 receptor 1 (IL-18R1), and IL-18 receptor accessory protein (IL-18RAP) were expressed at low levels (transcript per million (TPM) < 1), CCR5, CCR10, OSM receptor (OSMR), and leukemia


Fig. 1 Inflammatory receptors are present in the choroid plexus. **a** Schematic illustration of the inflammatory markers and their corresponding receptors. The inflammatory markers (green and blue circles) and their corresponding receptors (grey bars) are indicated by the black arrows. For OSM, the dotted black arrows indicate binding to IL-6ST in combination with either OSMR or LIFR. The illustration is based on the information provided in [67, 88, 102, 106]. **b** Expression of the inflammatory receptors in the rat and human choroid plexus. The expression levels were evaluated with RNA-seq and given in transcript per million (TPM). The human choroid plexus data was obtained from the GEO database, accession number GSE137619 [59]

Lolansen *et al. Fluids and Barriers of the CNS* (2021) 18:54

Page 7 of 15

inhibitory factor receptor (LIFR) at intermediate levels (1–5 TPM), and IL-6 signal transducer (IL-6ST) at high level (TPM = 39). Two inflammatory receptors targeted by the elevated inflammatory agents, CCR4 and CXCR1, were absent from the rat choroid plexus. To determine whether the rat choroid plexus expression levels were representative of that of humans, we compared our RNA-seq data with previously published RNA-seq choroid plexus data from humans (n = 6, age: 62 ± 6.1 y, 2 M/4 F, GEO database accession number GSE137619, https://www.ncbi.nlm.nih.gov/geo/query/acc.cgi?acc=GSE137619 [59], Fig. 1b). All inflammatory receptors targeted by the elevated inflammatory markers were expressed in the human choroid plexus. Hence, the only noticeable differences between humans and rats were absence of CCR4 and CXCR1 in the rat choroid plexus. Taken together, these data demonstrate choroidal expression of inflammatory receptors being targeted by the inflammatory markers found elevated in iNPH patients and thus support the notion that inflammatory markers can act directly on the choroid plexus and possibly modulate its functional properties.

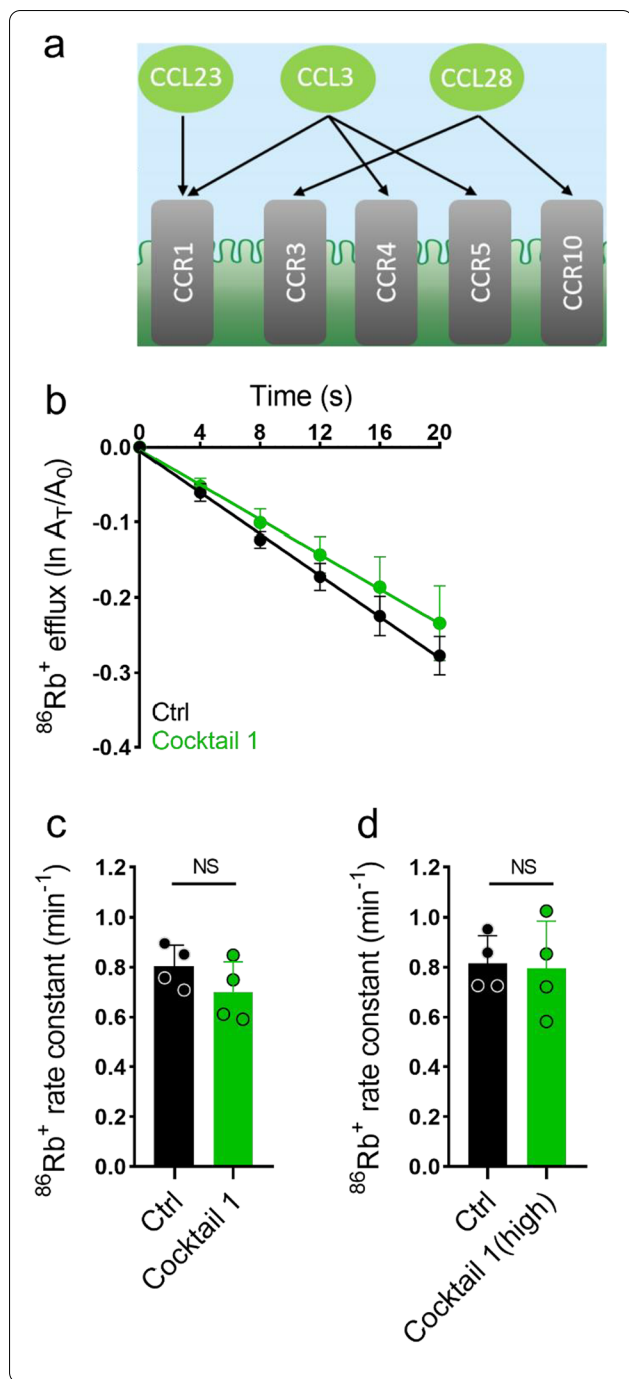### Inflammatory markers do not modulate NKCC1 activity in rat choroid plexus

To estimate the influence of the inflammatory markers that were elevated in iNPH patients on choroidal CSF secretion, we determined their effect on the activity of the choroidal water-transporting $Na^+/K^+/2Cl^-$ cotransporter NKCC1, a key contributor to choroidal CSF secretion [33, 41, 42]. To this end, we employed ex vivo rat choroid plexus exposed to the rat version of the respective inflammatory markers. As inflammatory markers may exert their effects on a longer time scale, the choroid plexus was placed in cell culture medium and incubated for 16 h in presence of the inflammatory markers. Each epithelial cell of the choroidal monolayer was thus directly in touch with the oxygenated and nutrient-rich culture medium, like individual cells in culture. The viability of the choroid plexus epithelial cells was confirmed with a calcein-AM survival assay (Fig. 2a–c), which demonstrated that the epithelial cells were viable at the end of the culturing period. The transport activity of NKCC1 in the 16 h cultured ex vivo choroid plexus was assessed by rubidium ($^{86}Rb^+$) efflux experiments, in which $^{86}Rb^+$ replaces K^+ at its binding site and acts as a tracer for the K^+ transport through NKCC1. Inclusion of the NKCC1-specific inhibitor bumetanide (20 μM) diminished the choroidal $^{86}Rb^+$ efflux by ~56% (Fig. 2d, n = 5, P = 0.0008), thus demonstrating that a large fraction of the $^{86}Rb^+$ efflux occurred via NKCC1 in this experimental set-up. The $^{86}Rb^+$ assay thus allows for direct assessment of the effect of the inflammatory markers on the choroidal NKCC1 activity.

The elevated inflammatory markers were grouped into two cocktails to determine their effect on NKCC1. Cocktail 1 contained the most significantly elevated inflammatory markers in the iNPH patient samples (CCL28, CCL23, CCL3; P < 0.001, Fig. 3a). As rat CCL6 is orthologous to human CCL23 [66], rat CCL6 was employed to mimic human CCL23 signaling. The $^{86}Rb^+$ efflux rate (read-out of NKCC1 transport activity) from the rat choroid plexus was not significantly altered by exposure to cocktail 1 (Fig. 3b, c, n = 4, P = 0.21), nor to
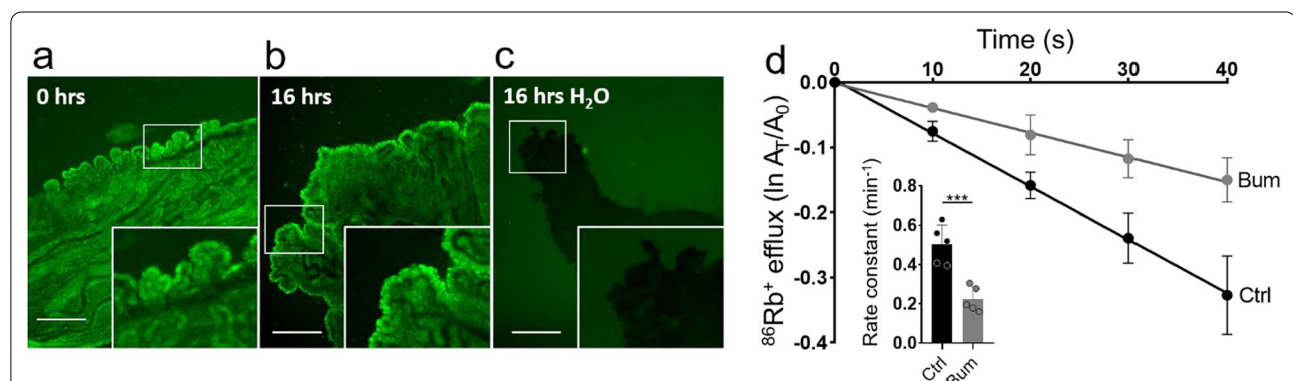
Fig. 2 The choroid plexus remains viable ex vivo. **a** Calcein-AM staining of choroid plexus directly after isolation (0 h). **b** Calcein-AM staining of choroid plexus after 16 h of incubation in cell culture medium (16 h). **c** Calcein-AM staining of choroid plexus after 16 h of incubation in sterile water (16 h H_2O), scale bars 500 μm. Inserts in **a-c** contain representative regions of the choroid plexus (white boxes) upon ×5 magnification. **d** $^{86}Rb^+$ efflux from the choroid plexus as a function of time in control solution (ctrl, n = 5) or in presence of 20 μM bumetanide (bum, n = 5). The y-axis represents the natural logarithm of the $^{86}Rb^+$ amount left in the choroid plexus at time T (A_T) divided by the initial amount at time 0 (A_0). Insert: $^{86}Rb^+$ efflux rate constant in control solution (0.50 ± 0.10 min^{-1}, n = 5) or in presence of 20 μM bumetanide (0.22 ± 0.06 min^{-1}, n = 5), P = 0.0008. Error bars in **d** represent standard deviation and statistical significance was tested with an unpaired two-tailed t-test. ***P < 0.001

Lolansen *et al. Fluids and Barriers of the CNS*   (2021) 18:54

Page 8 of 15

Fig. 3 The inflammatory markers CCL28, CCL23, and CCL3 do not modulate the NKCC1 activity. **a** Schematic illustration of the inflammatory markers in cocktail 1 (CCL28, CCL23, and CCL3) and their corresponding receptors. **b** $^{86}Rb^+$ efflux from the rat choroid plexus as a function of time in the control setting (black, n = 4) or with exposure to cocktail 1 (green, n = 4) containing CCL28 (100 ng/ml), CCL23 (200 ng/ml), and CCL3 (100 ng/ml). The y-axis represents the natural logarithm of the $^{86}Rb^+$ amount left in the choroid plexus at time T (A_T) divided by the initial amount at time 0 (A_0). **c** $^{86}Rb^+$ efflux rate constant in the control setting (0.80 ± 0.09 min^{-1}, n = 4) or with exposure to cocktail 1 (0.70 ± 0.12 min^{-1}, n = 4, CCL28 (100 ng/ml), CCL23 (200 ng/ml), and CCL3 (100 ng/ml). P = 0.21. **d** $^{86}Rb^+$ efflux rate constant in the control setting (0.82 ± 0.11 min^{-1}, n = 4) or with exposure to high concentrations of cocktail 1 (0.80 ± 0.19 min^{-1}, n = 4, CCL28 (500 ng/ml), CCL23 (500 ng/ml), and CCL3 (500 ng/ml), P = 0.86. Error bars in **b**, **c** and **d** represent standard deviation and statistical significance was tested with an unpaired two-tailed t-test. NS, not significant

n = 3–4, P = 0.32). As our RNA-seq analysis revealed absence of CCR4 and CXCR1 from the rat choroid plexus, signaling through these receptors was not investigated. Hence, none of the combinations of inflammatory markers found in the CSF from iNPH patients modulated the rat choroidal NKCC1 activity. Taken together, our findings demonstrate that although inflammatory markers are present at elevated levels in the CSF from iNPH patients, they do not directly alter the fraction of the choroidal CSF secretion predicted to be mediated by NKCC1 transport activity on the tested time scale.

Discussion

This study, based on the novel PEA technique, uncovers the inflammatory profile of the CSF from iNPH patients investigating the largest number of inflammatory markers so far and providing novel insight into the inflammatory marker profile of CSF from iNPH patients. We here demonstrate that the CSF from iNPH patients contains elevated levels of a subset of inflammatory markers. The corresponding inflammatory receptors are, in general, expressed in the choroid plexus of rats and humans, but their activation did not stimulate NKCC1 that is highly expressed in the luminal membrane of choroid plexus in mice, rats, and humans [41, 68, 69] and demonstrated to support approximately half of the CSF secreted in the tested species (mice, rats, dogs; [33, 41, 42]). Note that the NKCC1 inhibitor bumetanide only exerts its inhibitory action on NKCC1-mediated CSF secretion when delivered directly into the cerebral ventricles of the experimental animal (to target NKCC1 at the luminal membrane of choroid plexus [33, 41, 42]) and not upon administration of bumetanide i.v. or i.p., in which cases, the inhibitor fails to reach its choroidal target [70, 71].

excessively high concentrations of these (Fig. 3d, n = 4, P = 0.86). Cocktail 2 (IL-18, CXCL1, and OSM) targeted the remaining inflammatory receptors (Fig. 4a). Since CXCL1, CXCL2, and IL-8 activate the same receptors, CXCR1 and CXCR2 [67] (Fig. 1a), only one inflammatory marker, CXCL1, was chosen to activate these. Application of cocktail 2 (IL-18, CXCL1, and OSM) did not alter the $^{86}Rb^+$ efflux rate either (Fig. 4b, c, n = 3–4, P = 0.94), nor did the excessively high concentrations of these (Fig. 4d,
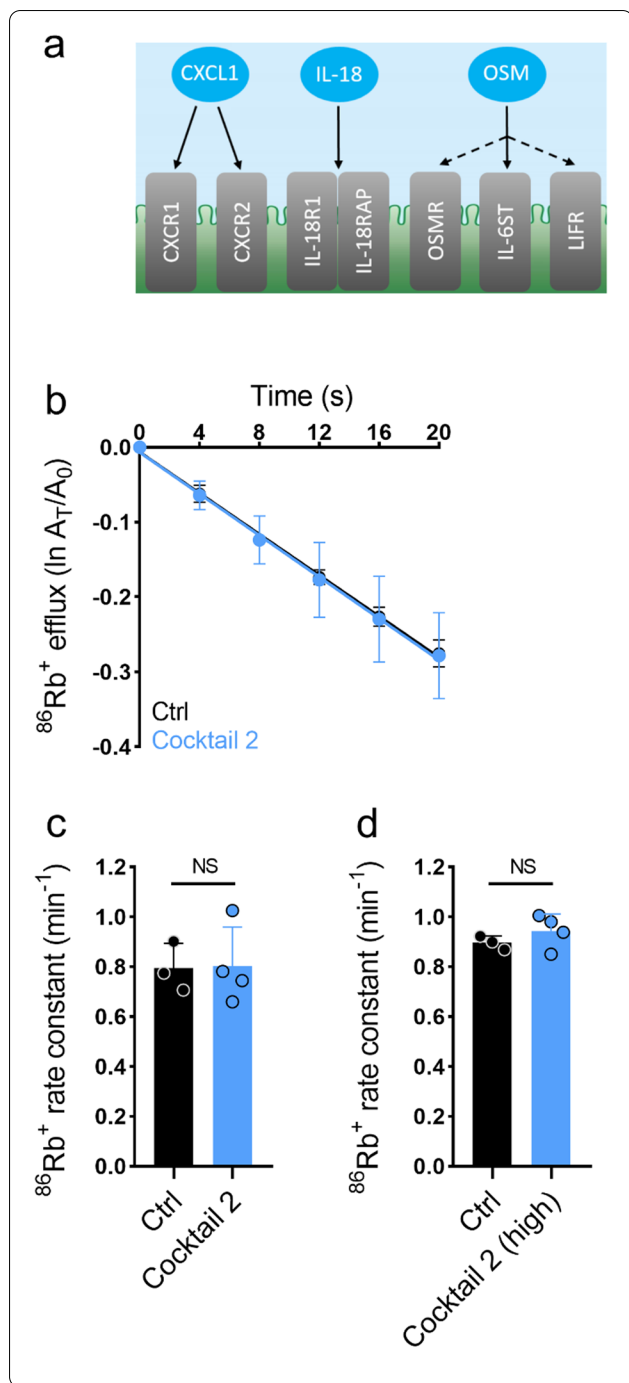
Fig. 4 The inflammatory markers IL-18, CXCL1, and OSM do not modulate the NKCC1 activity. **a** Schematic illustration of the inflammatory markers in cocktail 2 (IL-18, CXCL1, and OSM) and their corresponding receptors. **b** $^{86}Rb^+$ efflux from the rat choroid plexus as a function of time in the control setting (black, n = 3) or with exposure to cocktail 1 (blue, n = 4) containing IL-18 (200 ng/ml), CXCL1 (100 ng/ml), and OSM (200 ng/ml). The y-axis represents the natural logarithm of the $^{86}Rb^+$ amount left in the choroid plexus at time T (A_T) divided by the initial amount at time 0 (A_0). **c** $^{86}Rb^+$ efflux rate constant in the control setting (0.79 ± 0.10 min^{-1}, n = 3) or with exposure to cocktail 2 (0.80 ± 0.16 min^{-1}, n = 4) containing IL-18 (200 ng/ml), CXCL1 (100 ng/ml), and OSM (200 ng/ml). P = 0.94. **d** $^{86}Rb^+$ efflux rate constant in the control setting (0.90 ± 0.03 min^{-1}, n = 3) or with exposure to high concentrations of cocktail 2 (0.94 ± 0.07 min^{-1}, n = 4, IL-18 (500 ng/ml), CXCL1 (500 ng/ml), and OSM (500 ng/ml)), P = 0.32. Error bars in **b**–**d** represent standard deviation and statistical significance was tested with an unpaired two-tailed t-test. NS, not significant

Eleven inflammatory markers were elevated in CSF obtained from iNPH patients compared to elderly control subjects. Three inflammatory markers (OPG, 4E-BP1, and Flt3L) were not investigated experimentally, as they were unlikely to directly influence choroidal CSF secretion: OPG acts as a decoy receptor [72], 4E-BP1 represses translation and plays a predominant role in cell proliferation [73], while Flt3L, a hematopoietic growth factor, promotes differentiation of hematopoietic stem cells, particularly dendritic cells [74]. The remaining eight inflammatory markers were investigated for their ability to alter choroidal CSF secretion: CCL28, CCL23, CCL3, CXCL1, IL-18, IL-8, OSM and CXCL6.

CCL28 is a chemokine constitutively expressed by epithelial cells at mucosal sites [75], which promotes chemotaxis of immune cells through the receptors CCR3 and CCR10 [75, 76] and is inducible upon presence of inflammatory or infectious stimuli [77]. CCL28 is elevated in CSF from patients with Parkinson's disease (PD) [78], who have normal CSF production [79], and its presence in iNPH patients may instead indicate similar pathological features of neurodegeneration and/or inflammation [80]. The chemokine CCL23 is expressed mainly by macrophages and exerts its chemotactic effects on immune cells through CCR1 [81, 82]. Elevated CCL23 levels are reported in various inflammatory diseases [83, 84] and is, in addition, associated with progression from mild cognitive impairment to Alzheimer's disease (AD) [85]. Elevated CCL23 in both AD and iNPH aligns well with the overlapping clinical characteristics of iNPH and AD [86] and the concomitant AD pathology found in iNPH [87]. CCL3 is a chemokine that exerts its proinflammatory actions through the receptors CCR1 and CCR5, and with less affinity through CCR4 [88]. CCL3 is secreted

Inflammatory markers therefore appear *not* to promote iNPH via induction of choroidal CSF hypersecretion by promotion of NKCC1 activation, at least not in the rat ex vivo model here employed. Based on the present data set, however, we cannot rule out that other transport mechanisms involved in CSF secretion (see [71] for review) could be modulated by these inflammatory agents.

Lolansen *et al. Fluids and Barriers of the CNS*   (2021) 18:54

Page 10 of 15

by various cells such as monocytes, macrophages, and epithelial cells [89] and is inducible by proinflammatory agents such as lipopolysaccharides, tumor necrosis factor α, and IL-1β [90, 91]. CCL3 is elevated in CSF from patients with posthemorrhagic hydrocephalus [92] and hydrocephalus associated with tuberculous meningitis [93], which both associate with inflammation [94]. Elevated CCL3 in iNPH patients suggests similar inflammatory conditions in this patient group.

The chemokines CXCL1, CXCL6, and IL-8 exert their actions through the receptors CXCR1 and CXCR2 [67]. CXCL1 is elevated in brain tissue from hydrocephalic mice with genetically induced ciliary dysfunction, in which hydrocephalus develops concurrent with neuroinflammation and tissue injury [95]. As no antecedent proinflammatory insult occurs in these mice, the authors conclude that neuroinflammation arises as a consequence of the intracranial changes associated with hydrocephalus development [95]. Elevated CXCL1 in iNPH patients may therefore reflect presence of neuroinflammation and it may arise concomitantly with development of hydrocephalus. Like CXCL1, CXCL6 serves as a neutrophil chemoattractant [96] and is elevated in bacterial and viral meningitis [97].

Several studies have investigated the proinflammatory chemokine IL-8 in relation to hydrocephalus. While some studies report elevated IL-8 in CSF from patients with different hydrocephalic conditions [93, 98, 99], others report unaltered levels [92, 98–101]. Our findings of elevated IL-8 in CSF from iNPH patients are in agreement with the findings by Czubowicz [98] but contradict others [99–101]. Although the contradicting findings may result from methodological differences, additional studies are required to determine whether elevated CSF levels of IL-8 are characteristic of iNPH. IL-18 is a proinflammatory cytokine released in response to inflammatory and infectious stimuli which signals through the receptors IL-18R1 and IL-18RAP and is involved in various neurological conditions [102]. IL-18 is elevated in CSF from preterm infants with posthemorrhagic hydrocephalus and hydrocephalus associated with spina bifida and aqueductal stenosis [103, 104]. As these conditions are associated with inflammatory changes including astrogliosis, microgliosis, and white matter damage [94, 103–105], it can be speculated whether similar changes occur in iNPH patients.

OSM is a pleiotropic interleukin-6-type cytokine that utilizes two receptor complexes, IL-6ST/LIFR and IL-6ST/OSMR, to mediate a broad range of homeostatic activities, some of which include hematopoiesis, liver regeneration, and homeostasis of neural precursor cells [106, 107]. Overproduction of OSM is associated with

skin and airway inflammation, inflammatory bowel disease, and other pathological conditions [106, 108, 109]. OSM was recently identified as a potential CSF marker of general CNS inflammation, although interestingly, the study included iNPH patients and patients with idiopathic intracranial hypertension as the non-inflamed controls [110]. The elevated OSM levels in CSF from iNPH patients in the present study are indicative of inflammation, but the inflammatory condition may be less pronounced in comparison to other patient groups with prominent signs of inflammation such as those suffering from meningitis or subarachnoid hemorrhage [110].

One inflammatory marker, CDCP1, was significantly decreased in the CSF obtained from iNPH patients compared to elderly control subjects. CDCP1 is a transmembrane glycoprotein chemotactic for T-cells [65] that has been associated with cell adhesion and cancer development [111]. Although its physiological role in iNPH patients remains unclear, it can be speculated whether CDCP1 may serve as a diagnostic marker, potentially distinguishing iNPH from other types of hydrocephalus.

Inflammatory markers such as cytokines, interleukins, and chemokines signal through various intracellular pathways and are capable of acting synergistically or antagonistically [112]. In the present study, the elevated inflammatory markers were combined into cocktails and the ability of the inflammatory markers to modulate choroidal CSF secretion was thus not assessed individually. The combination of the inflammatory markers into cocktails may have compromised the effect of each inflammatory marker. However, as the inflammatory markers were elevated collectively in the CSF from iNPH patients, we sought to mimic the nature of iNPH by combining the inflammatory markers. In the present study, we did not obtain evidence that inflammatory markers can act directly on the choroid plexus to promote such hyperactivation of NKCC1, as was observed in an in vivo rodent model of intraventricular hemorrhage [33]. The excised choroid plexuses were kept in tissue culture conditions for 16 h to allow the inflammatory agents to serve their purpose via modulation of transcriptional and translational processes, including post-translational modifications such as phosphorylation of proteins, which has been described earlier for NKCC1-mediated CSF hypersecretion [33]. However, it is possible that all elevated inflammatory markers have to be included in the same experiment, that additional time is required for the inflammatory markers to have an effect on the choroidal transport protein NKCC1 (and/or target other choroidal transporters), or that lesser time is required for optimal initiation of the inflammatory machinery: Other studies

Lolansen *et al. Fluids and Barriers of the CNS*   (2021) 18:54

Page 11 of 15

have shown that upon an inflammatory stimulus, the choroid plexus transcriptome responds rapidly within 3–6 h [113, 114] followed by gradual return to baseline within 72 h [113]. However, whereas these studies only applied an inflammatory stimulus once, we exposed the choroid plexus to the inflammatory markers continuously for 16 h and would therefore not expect the effects of the inflammatory markers on the choroidal CSF secretion to subside. Although we document choroid plexus epithelial cell viability and bumetanide-sensitive $^{86}Rb^+$ efflux following the 16 h incubation time, prolonged presence of the inflammatory markers may have initiated oxidative stress, apoptosis, or other cellular mechanisms that could have compromised potential effects of the inflammatory markers on choroidal NKCC1-mediated ion transport. However, other research groups have reported successful exposure of choroid plexus epithelial cell lines to inflammatory stimuli for longer time periods [115].

The inability of the inflammatory markers to modulate choroidal NKCC1 transport activity ex vivo and thus potentially contribute to development of iNPH leaves the molecular coupling between inflammatory markers and iNPH unresolved. Elevated levels of inflammatory markers in CSF from iNPH patients indicate presence of an ongoing inflammatory condition. However, whether this inflammatory condition promotes iNPH development or arises secondarily to the pathological changes observed in the iNPH brain remains uncertain. Some studies demonstrate that CSF levels of inflammatory markers decrease following CSF shunting in parallel with clinical improvement [116, 117] suggesting that the inflammatory condition is intrinsically related to disturbed CSF dynamics. Interestingly, we did not find any significant differences in the CSF distribution of inflammatory markers when comparing iNPH shunt responders and iNPH shunt non-responders. Our findings therefore illustrate that the inflammatory profile of iNPH patient CSF obtained during the diagnostic workup cannot be used to predict the outcome of VP shunting in this patient group. One must, however, bear in mind that shunt response may be affected by other factors not accounted for in the present study, including clinical complications and comorbidities. In the future, studies should aim to resolve the role of inflammation in the pathogenesis of iNPH and thereby elucidate whether alleviation of the inflammation condition may prove beneficial in treatment of iNPH.

The present study is associated with certain limitations. Although all included iNPH patients were in moderate to severe stage of disease (see "Methods"), the exact time between onset of symptoms and time of CSF sampling is unknown and could affect the inflammatory profile of the patients. The elderly control group is of an average

age of 10 years below that of the iNPH patients. Since inflammation tends to increase with age, such age difference could affect the obtained results. We quantified the inflammatory marker content in CSF from human iNPH patients sampled at one time point only. Since an animal model of iNPH does not currently exist, the ability of (the rat version of) these elevated inflammatory markers to modulate choroidal NKCC1 activity was investigated in rat choroid plexus, as these experiments would not be possible with human tissue. Although our RNA-seq analysis revealed that the majority of the corresponding inflammatory receptors were expressed in the choroid plexus of rats and humans, we cannot exclude that differences between species (humans and rats) may have compromised the findings of our study. Direct modulation of choroidal CSF secretion requires that the receptors for the elevated inflammatory markers are present on the CSF-facing membrane of the choroid plexus. As our RNA-seq analysis only allowed for determination of choroidal receptor expression, not membrane localization, we cannot exclude that some of the inflammatory receptors were absent from the CSF-facing membrane and thus not activated by inclusion of the respective inflammatory marker.

Conclusion

Here, we demonstrate that the CSF from iNPH patients contains elevated levels of a subset of inflammatory markers. Although the corresponding inflammatory receptors are, in general, expressed in the choroid plexus of rats and humans, their activation did not modulate the activity of the NKCC1 transport mechanism that is key in the CSF-secreting molecular machinery. Inflammation may possibly modulate other CSF-secreting transport mechanisms expressed in choroid plexus or other proposed CSF-secreting barriers, i.e. the endothelium or the ependymal cell layer. Unravelling of the molecular mechanisms underlying the pathological CSF accumulation seen in iNPH patients, and its relation to the inflammatory marker profile observed in this patient group, therefore awaits future research efforts.

Lolansen *et al. Fluids and Barriers of the CNS*   (2021) 18:54

Page 12 of 15

Supplementary Information

Additional file 1: Table S1. Inflammatory markers from Olink's inflammation panel (Art. No. 95301). This table provides an overview of the inflammatory markers included in Olink's inflammation panel and highlights the inflammatory markers excluded from the statistical analysis of the CSF samples

Additional file 2: Table S2. Statistical tests and results for the comparison of inflammatory markers levels iNPH patients and elderly control subjects.

Additional file 3: Table S3. Statistical tests and results for the comparison of inflammatory markers levels in iNPH responders and iNPH non-responders.

Authors' contributions
SDL, NR, AHS, MJ, and NM designed the research study; AHS and SGH provided CSF samples and the clinical analysis of study participants. SDL, NR, and SNA handled CSF samples, executed experiments and/or analyzed data. SDL and NM drafted the manuscript. All authors read and approved the final manuscript.

Availability of data and materials
The datasets used and/or analyzed during the current study are available from the corresponding author on reasonable request. The human choroid plexus data that supports the findings of this study are available in the GEO database, accession number GSE137619, https://www.ncbi.nlm.nih.gov/geo/query/acc.cgi?acc=GSE137619 [59].

Declarations

Ethics approval and consent to participate
Written informed consent was obtained from all patients and control subjects included in the study. The study was approved by the Ethics committee of the Capital Region of Denmark (H-18046630). Animal experiments were in compliance with the European Community Council Directive 2010/63/EU on the Protection of Animals used for Scientific Purposes.

Consent for publication
Not applicable.

Competing interests
The authors declare that they have no competing interests.

Author details
[1]Department of Neuroscience, University of Copenhagen, Blegdamsvej 3B, 2200 Copenhagen, Denmark. [2]Department of Neurosurgery, Rigshospitalet, Copenhagen, Denmark. [3]Danish Dementia Research Centre, Department of Neurology, Rigshospitalet, Copenhagen, Denmark.

References

1. Hakim S, Adams RD. The special clinical problem of symptomatic hydrocephalus with normal cerebrospinal fluid pressure. J Neurol Sci. 1965;2:307–27.
2. Jaraj D, Rabiei K, Marlow T, Jensen C, Skoog I, Wikkelso C. Prevalence of idiopathic normal-pressure hydrocephalus. Neurology. 2014;82:1449–54.
3. Andersson J, Rosell M, Kockum K, Lilja-Lund O, Söderström L, Laurell K. Prevalence of idiopathic normal pressure hydrocephalus: a prospective, population based study. PLoS ONE. 2019;14:e0217705.
4. Relkin N, Marmarou A, Klinge P, Bergsneider M, Black PM. Diagnosing idiopathic normal-pressure hydrocephalus. Neurosurgery. 2005;57:S4-16 (**discussion ii-v**).
5. Hebb AO, Cusimano MD. Idiopathic normal pressure hydrocephalus: a systematic review of diagnosis and outcome. Neurosurgery. 2001;49:1166–86.
6. Mori K. Management of idiopathic normal-pressure hydrocephalus: a multiinstitutional study conducted in Japan. J Neurosurg. 2001;95:970–3.
7. McGirt MJ, Woodworth G, Coon AL, Thomas G, Williams MA, Rigamonti D. Diagnosis, treatment, and analysis of long-term outcomes in idiopathic normal-pressure hydrocephalus. Neurosurgery. 2005;57:699–705.
8. Marmarou A, Young HF, Aygok GA, Sawauchi S, Tsuji O, Yamamoto T, et al. Diagnosis and management of idiopathic normal-pressure hydrocephalus: a prospective study in 151 patients. J Neurosurg. 2005;102:987–97.
9. Eide PK, Sorteberg W. Outcome of surgery for idiopathic normal pressure hydrocephalus: role of preoperative static and pulsatile intracranial pressure. World Neurosurg. 2016;86:186-193.e1.
10. Eide PK, Sorteberg W. Diagnostic intracranial pressure monitoring and surgical management in idiopathic normal pressure hydrocephalus: a 6-Year review of 214 patients. Neurosurgery. 2010;66:80–91.
11. Eide PK. Intracranial pressure parameters in idiopathic normal pressure hydrocephalus patients treated with ventriculo-peritoneal shunts. Acta Neurochir. 2006;148:21–9.
12. Jacobsson J, Qvarlander S, Eklund A, Malm J. Comparison of the CSF dynamics between patients with idiopathic normal pressure hydrocephalus and healthy volunteers. J Neurosurg. 2019;131:1018–23.
13. Lindstrom EK, Ringstad G, Mardal KA, Eide PK. Cerebrospinal fluid volumetric net flow rate and direction in idiopathic normal pressure hydrocephalus. Neuroimage Clin. 2018;20:731–41.
14. Albeck MJ, Borgesen SE, Gjerris F, Schmidt JF, Sorensen PS. Intracranial pressure and cerebrospinal fluid outflow conductance in healthy subjects. J Neurosurg. 1991;74:597–600.
15. Malm J, Jacobsson J, Birgander R, Eklund A. Reference values for CSF outflow resistance and intracranial pressure in healthy elderly. Neurology. 2011;76:903–9.
16. Norager NH, Olsen MH, Pedersen SH, Riedel CS, Czosnyka M, Juhler M. Reference values for intracranial pressure and lumbar cerebrospinal fluid pressure: a systematic review. Fluids Barriers CNS. 2021;18:19.
17. Williams MA, Malm J. Diagnosis and treatment of idiopathic normal pressure hydrocephalus. Contin. 2016;22:579–99.
18. Eide PK, Fremming AD, Sorteberg A. Lack of relationship between resistance to cerebrospinal fluid outflow and intracranial pressure in normal pressure hydrocephalus. Acta Neurol Scand. 2003;108:381–8.
19. Wikkelso C, Hellström P, Klinge PM, Tans JTJ. The European iNPH Multicentre Study on the predictive values of resistance to CSF outflow and the CSF Tap Test in patients with idiopathic normal pressure hydrocephalus. J Neurol Neurosurg Psychiatry. 2013;84:562–8.
20. Gideon P, Staahlberg F, Thomsen C, Gjerris F, Sorensen PS, Henriksen O. Cerebrospinal fluid flow and production in patients with normal pressure hydrocephalus studied by MRI. Neuroradiology. 1994;36:210–5.
21. Luetmer PH, Huston J, Friedman JA, Dixon GR, Petersen RC, Jack CR, et al. Measurement of cerebrospinal fluid flow at the cerebral aqueduct by use of phase-contrast magnetic resonance imaging: technique validation and utility in diagnosing idiopathic normal pressure hydrocephalus. Neurosurgery. 2002;50:534–43.

Lolansen *et al. Fluids and Barriers of the CNS*   (2021) 18:54

Page 13 of 15

22. He WJ, Zhou X, Long J, Xu QZ, Huang XJ, Jiang J, et al. Idiopathic normal pressure hydrocephalus and elderly acquired hydrocephalus: evaluation with cerebrospinal fluid flow and ventricular volume parameters. Front Aging Neurosci. 2020;12:584842.

23. Yin LK, Zheng JJ, Zhao L, Hao XZ, Zhang XX, Tian JQ, et al. Reversed aqueductal cerebrospinal fluid net flow in idiopathic normal pressure hydrocephalus. Acta Neurol Scand. 2017;136:434–9.

24. Aslan K, Tokatlioglu O, Aydin R, Polat AV, Incesu L. Normal pressure hydrocephalus versus atrophic dilatation to distinguish and predict the benefits of surgical intervention with a phase-contrast MRI technique. Turk Neurosurg. 2014;24:525–31.

25. Schroth G, Klose U. MRI of CSF flow in normal pressure hydrocephalus. Psychiatry Res. 1989;29:289–90.

26. Takizawa K, Matsumae M, Hayashi N, Hirayama A, Yatsushiro S, Kuroda K. Hyperdynamic CSF motion profiles found in idiopathic normal pressure hydrocephalus and Alzheimer's disease assessed by fluid mechanics derived from magnetic resonance images. Fluids Barriers CNS. 2017;14:29.

27. Bradley WG, Kortman KE, Burgoyne B. Flowing cerebrospinal fluid in normal and hydrocephalic states: appearance on MR images. Radiology. 1986;159:611–6.

28. Bateman GA, Loiselle AM. Can MR measurement of intracranial hydrodynamics and compliance differentiate which patient with idiopathic normal pressure hydrocephalus will improve following shunt insertion? Acta Neurochir. 2007;149:455–62.

29. Mase M, Miyati T, Kasai H, Demura K, Osawa T, Hara M, et al. Noninvasive estimation of intracranial compliance in idiopathic NPH using MRI. Acta Neurochir Suppl. 2008;102:115–8.

30. Eisenberg HM, McComb JG, Lorenzo AV. Cerebrospinal fluid overproduction and hydrocephalus associated with choroid plexus papilloma. J Neurosurg. 1974;40:381–5.

31. Hallaert GG, Vanhauwaert DJ, Logghe K, Van den Broecke C, Baert E, Van Roost D, et al. Endoscopic coagulation of choroid plexus hyperplasia. J Neurosurg Pediatr. 2012;9:169–77.

32. Trevisi G, Frassanito P, di Rocco C. Idiopathic cerebrospinal fluid overproduction: case-based review of the pathophysiological mechanism implied in the cerebrospinal fluid production. Croat Med J. 2014;55:377–87.

33. Karimy JK, Zhang J, Kurland DB, Theriault BC, Duran D, Stokum JA, et al. Inflammation-dependent cerebrospinal fluid hypersecretion by the choroid plexus epithelium in posthemorrhagic hydrocephalus. Nat Med. 2017;23:997–1003.

34. Lolansen SD, Rostgaard N, Oernbo EK, Juhler M, Simonsen AH, MacAulay N. Inflammatory markers in cerebrospinal fluid from patients with hydrocephalus: a systematic literature review. Dis Markers. 2021;2021:1–12.

35. Chaudhry SR, Stoffel-Wagner B, Kinfe TM, Güresir E, Vatter H, Dietrich D, et al. Elevated systemic IL-6 levels in patients with aneurysmal subarachnoid hemorrhage is an unspecific marker for post-SAH complications. Int J Mol Sci. 2017;18:2580.

36. Lenski M, Biczok A, Huge V, Forbrig R, Briegel J, Tonn JC, et al. Role of cerebrospinal fluid markers for predicting shunt-dependent hydrocephalus in patients with subarachnoid hemorrhage and external ventricular drain placement. World Neurosurg. 2019;121:e535–42.

37. Lv S, Wu Q, Liu J, Shao J, Wen L, Xue J, et al. Levels of interleukin-1β, interleukin-18, and tumor necrosis factor-α in cerebrospinal fluid of aneurysmal subarachnoid hemorrhage patients may be predictors of early brain injury and clinical prognosis. World Neurosurg. 2018;111:e362–73.

38. Whitelaw A, Christie S, Pople I. Transforming growth factor-β1: a possible signal molecule for posthemorrhagic hydrocephalus? Pediatr Res. 1999;46:576.

39. Schürkämper M, Medele R, Zausinger S, Schmid-Elsaesser R, Steiger HJ. Dexamethasone in the treatment of subarachnoid hemorrhage revisited: a comparative analysis of the effect of the total dose on complications and outcome. J Clin Neurosci. 2004;11:20–4.

40. Thwaites GE, Macmullen-Price J, Chau TTH, Phuong Mai P, Dung NT, Simmons CP, et al. Serial MRI to determine the effect of dexamethasone on the cerebral pathology of tuberculous meningitis: an observational study. Lancet Neurol. 2007;6:230–6.

41. Steffensen AB, Oernbo EK, Stoica A, Gerkau NJ, Barbuskaite D, Tritsaris K, et al. Cotransporter-mediated water transport underlying cerebrospinal fluid formation. Nat Commun. 2018;9:2167.

42. Javaheri S, Wagner K. Bumetanide decreases canine cerebrospinal fluid production. In vivo evidence for NaCl cotransport in the central nervous system. J Clin Investig. 1993;92:2257–61.

43. Hellström P, Klinge P, Tans J, Wikkelsoe C. A new scale for assessment of severity and outcome in iNPH. Acta Neurol Scand. 2012;126:229–37.

44. Folstein M, Folstein S, McHugh P. "Mini-mental state". A practical method for grading the cognitive state of patients for the clinician. J Psychiatr Res. 1975;12:189–98.

45. McKhann GM, Knopman DS, Chertkow H, Hyman BT, Jack CR, Kawas CH, et al. The diagnosis of dementia due to Alzheimer's disease: recommendations from the national institute on aging-Alzheimer's association workgroups on diagnostic guidelines for Alzheimer's disease. Alzheimer's Dement. 2011;7:263–9.

46. Albert MS, DeKosky ST, Dickson D, Dubois B, Feldman HH, Fox NC, et al. The diagnosis of mild cognitive impairment due to Alzheimer's disease: recommendations from the National Institute on Aging-Alzheimer's Association workgroups on diagnostic guidelines for Alzheimer's disease. Alzheimer's Dement. 2011;7:270–9.

47. Del Campo M, Mollenhauer B, Bertolotto A, Engelborghs S, Hampel H, Simonsen AH, et al. Recommendations to standardize preanalytical confounding factors in Alzheimers and Parkinsons disease cerebrospinal fluid biomarkers: an update. Biomark Med. 2012;6:419–30.

48. Assarsson E, Lundberg M, Holmquist G, Björkesten J, Thorsen SB, Ekman D, et al. Homogenous 96-plex PEA immunoassay exhibiting high sensitivity, specificity, and excellent scalability. PLoS ONE. 2014;9:e95192.

49. Kilkenny C, Browne W, Cuthill IC, Emerson M, Altman DG. Animal research: reporting in vivo experiments: the ARRIVE guidelines. Br J Pharmacol. 2010;160:1577–9.

50. Uggeri J, Gatti R, Belletti S, Scandroglio R, Corradini R, Rotoli B, et al. Calcein-AM is a detector of intracellular oxidative activity. Histochem Cell Biol. 2004;122:499–505.

51. Keep RF, Xiang J, Betz AL. Potassium cotransport at the rat choroid plexus. Am J Physiol - Cell Physiol. 1994;267:C1616–22.

52. GitHub, MacAulay lab. RNA sequencing scripts. https://github.com/Sorennorge/MacAulayLab-RNAseq1. Accessed 20 June 2021.

53. Dobin A, Davis CA, Schlesinger F, Drenkow J, Zaleski C, Jha S, et al. STAR: ultrafast universal RNA-seq aligner. Bioinformatics. 2013;29:15–21.

54. Abrams ZB, Johnson TS, Huang K, Payne PRO, Coombes K. A protocol to evaluate RNA sequencing normalization methods. BMC Bioinform. 2019;20:679.

55. Li B, Dewey CN. RSEM: accurate transcript quantification from RNA-Seq data with or without a reference genome. BMC Bioinform. 2011;12:323.

56. Xin J, Mark A, Afrasiabi C, Tsueng G, Juchler M, Gopal N, et al. High-performance web services for querying gene and variant annotation. Genome Biol. 2016;17:91.

57. Wu C, MacLeod I, Su AI. BioGPS and MyGene.info: organizing online, gene-centric information. Nucleic Acids Res. 2013;41:D561–5.

58. My Gene Info. https://mygene.info. Accessed 15 June 2021.

59. Human choroid plexus data available at the Gene Expression Omnibus database. https://www.ncbi.nlm.nih.gov/geo/query/acc.cgi?acc=GSE137619. Accessed 15 May 2021.

60. Babraham Bioinformatics. Babraham Institute. http://www.bioinformatics.babraham.ac.uk/projects/fastqc. Accessed 15 June 2021.

61. Bolger AM, Lohse M, Usadel B. Trimmomatic: a flexible trimmer for Illumina sequence data. Bioinformatics. 2014;30:2114–20.

62. Bergman J, Svenningsson A, Liv P, Bergenheim T, Burman J. Location matters: highly divergent protein levels in samples from different CNS compartments in a clinical trial of rituximab for progressive MS. Fluids Barriers CNS. 2020;17:49.

63. Hughes CE, Nibbs RJB. A guide to chemokines and their receptors. FEBS J. 2018;285:2944–71.

64. Kany S, Vollrath JT, Relja B. Cytokines in inflammatory disease. Int J Mol Sci. 2019;20:6008.

65. Enyindah-Asonye G, Li Y, Ruth JH, Spassov DS, Hebron KE, Zijlstra A, et al. CD318 is a ligand for CD6. PNAS. 2017;114:E6912–21.

Lolansen *et al. Fluids and Barriers of the CNS*   (2021) 18:54

Page 14 of 15

66. Nomiyama H, Egami K, Tanase S, Miura R, Hirakawa H, Kuhara S, et al. Comparative DNA sequence analysis of mouse and human CC chemokine gene clusters. J Interferon Cytokine Res. 2003;23:37–45.

67. Zlotnik A, Yoshie O, Nomiyama H. The chemokine and chemokine receptor superfamilies and their molecular evolution. Genome Biol. 2006;7:243.

68. Praetorius J, Nielsen S. Distribution of sodium transporters and aquaporin-1 in the human choroid plexus. Am J Physiol Cell Physiol. 2006;291:C59-67.

69. Plotkin M, Kaplan M, Peterson L, Gullans S, Hebert S, Delpire E. Expression of the Na(+)-K(+)-2Cl- cotransporter BSC2 in the nervous system. Am J Physiol. 1997;272:C173-183.

70. Bothwell S, Omileke D, Patabendige A, Spratt N. CSF secretion is not altered by NKCC1 nor TRPV4 antagonism in healthy rats. Brain Sci. 2021;11:1117.

71. MacAulay N. Molecular mechanisms of brain water transport. Nat Rev Neurosci. 2021;22:326–44.

72. De Voogd FA, Gearry RB, Mulder CJ, Day AS. Osteoprotegerin: a novel biomarker for inflammatory bowel disease and gastrointestinal carcinoma. J Gastroenterol Hepatol. 2016;31:1386–92.

73. Qin X, Jiang B, Zhang Y. 4E-BP1, a multifactor regulated multifunctional protein. Cell Cycle. 2016;15:781–6.

74. Ramos MI, Tak PP, Lebre MC. Fms-like tyrosine kinase 3 ligand-dependent dendritic cells in autoimmune inflammation. Autoimmun Rev. 2014;13:117–24.

75. Pan J, Kunkel EJ, Gosslar U, Lazarus N, Langdon P, Broadwell K, et al. Cutting edge: a novel chemokine ligand for CCR10 And CCR3 expressed by epithelial cells in mucosal tissues. J Immunol. 2000;165:2943–9.

76. Mohan T, Deng L, Wang BZ. CCL28 chemokine: An anchoring point bridging innate and adaptive immunity. Int Immunopharmacol. 2017;51:165–70.

77. Ogawa H, Iimura M, Eckmann L, Kagnoff MF. Regulated production of the chemokine CCL28 in human colon epithelium. Am J Physiol Gastrointest Liver Physiol. 2004;287:G1062–9.

78. Santaella A, Kuiperij HB, Van Rumund A, Esselink RAJ, Van Gool AJ, Bloem BR, et al. Inflammation biomarker discovery in Parkinson's disease and atypical parkinsonisms. BMC Neurol. 2020;20:26.

79. Silverberg GD, Heit G, Huhn S, Jaffe RA, Chang SD, Bronte-Stewart H, et al. The cerebrospinal fluid production rate is reduced in dementia of the Alzheimer's type. Neurology. 2001;57:1763–6.

80. Molde K, Söderström L, Laurell K. Parkinsonian symptoms in normal pressure hydrocephalus: a population-based study. J Neurol. 2017;264:2141–8.

81. Patel VP, Kreider BL, Li Y, Li H, Leung K, Salcedo T, et al. Molecular and functional characterization of two novel human C-C chemokines as inhibitors of two distinct classes of myeloid progenitors. J Exp Med. 1997;185:1163–72.

82. Youn B, Zhang SM, Broxmeyer HE, Cooper S, Antol K, Fraser M, et al. Characterization of CKβ8 and CKβ8-1: two alternatively spliced forms of human β-chemokine, chemoattractants for neutrophils, monocytes, and lymphocytes, and potent agonists at CC chemokine receptor 1. Blood. 1998;91:3118–26.

83. Yanaba K, Yoshizaki A, Muroi E, Ogawa F, Asano Y, Kadono T, et al. Serum CCL23 levels are increased in patients with systemic sclerosis. Arch Dermatol Res. 2011;303:29–34.

84. Rioja I, Hughes FJ, Sharp CH, Warnock LC, Montgomery DS, Akil M, et al. Potential novel biomarkers of disease activity in rheumatoid arthritis patients: CXCL13, CCL23, transforming growth factor α, tumor necrosis factor receptor superfamily member 9, and macrophage colony-stimulating factor. Arthritis Rheum. 2008;58:2257–67.

85. Faura J, Bustamante A, Penalba A, Giralt D, Simats A, Martínez-Sáez E, et al. CCL23: a chemokine associated with progression from mild cognitive impairment to Alzheimer's disease. J Alzheimer's Dis. 2020;73:1585–95.

86. Di Ieva A, Valli M, Cusimano MD. Distinguishing Alzheimer's disease from normal pressure hydrocephalus: a search for MRI biomarkers. J Alzheimer's Dis. 2014;38:331–50.

87. Müller-Schmitz K, Krasavina-Loka N, Yardimci T, Lipka T, Kolman AGJ, Robbers S, et al. Normal pressure hydrocephalus associated with Alzheimer's disease. Ann Neurol. 2020;88:703–11.

88. White GE, Iqbal AJ, Greaves DR. CC chemokine receptors and chronic inflammation-therapeutic opportunities and pharmacological challenges. Pharmacol Rev. 2013;65:47–89.

89. Schaller TH, Batich KA, Suryadevara CM, Desai R, Sampson JH. Chemokines as adjuvants for immunotherapy: implications for immune activation with CCL3. Expert Rev Clin Immunol. 2017;13:1049–60.

90. Peterson PK, Hu S, Salak-Johnson J, Molitor TW, Chao CC. Differential production of and migratory response to β chemokines by human microglia and astrocytes. J Infect Dis. 1997;175:478–81.

91. Zhu X, Wei D, Chen O, Zhang Z, Xue J, Huang S, et al. Upregulation of CCL3/MIP-1alpha regulated by MAPKs and NF-kappaB mediates microglial inflammatory response in LPS-induced brain injury. Acta Neurobiol Exp. 2016;76:304–17.

92. Habiyaremye G, Morales DM, Morgan CD, McAllister JP, CreveCoeur TS, Han RH, et al. Chemokine and cytokine levels in the lumbar cerebrospinal fluid of preterm infants with post-hemorrhagic hydrocephalus. Fluids Barriers CNS. 2017;14:35.

93. Rohlwink UK, Mauff K, Wilkinson KA, Enslin N, Wegoye E, Wilkinson RJ, et al. Biomarkers of cerebral injury and inflammation in pediatric tuberculous meningitis. Clin Infect Dis. 2017;65:1298–307.

94. Karimy JK, Reeves BC, Damisah E, Duy PQ, Antwi P, David W, et al. Inflammation in acquired hydrocephalus: pathogenic mechanisms and therapeutic targets. Nat Rev Neurol. 2020;16:285–96.

95. Goulding DS, Caleb Vogel R, Pandya CD, Shula C, Gensel JC, Mangano FT, et al. Neonatal hydrocephalus leads to white matter neuroinflammation and injury in the corpus callosum of Ccdc39 hydrocephalic mice. J Neurosurg Pediatr. 2020;25:476–83.

96. Wuyts A, Van Osselaer N, Haelens A, Samson I, Herdewijn P, Ben-Baruch A, et al. Characterization of synthetic human granulocyte chemotactic protein 2: usage of chemokine receptors CXCR1 and CXCR2 and in vivo inflammatory properties. Biochemistry. 1997;36:2716–23.

97. Lepennetier G, Hracsko Z, Unger M, Van Griensven M, Grummel V, Krumbholz M, et al. Cytokine and immune cell profiling in the cerebrospinal fluid of patients with neuro-inflammatory diseases. J Neuroinflammation. 2019;16:219.

98. Czubowicz K, Głowacki M, Fersten E, Kozłowska E, Strosznajder RP, Czernicki Z. Levels of selected pro- and anti-inflammatory cytokines in cerebrospinal fluid in patients with hydrocephalus. Folia Neuropathol. 2017;55:301–7.

99. Killer M, Arthur A, Al-Schameri AR, Barr J, Elbert D, Ladurner G, et al. Cytokine and growth factor concentration in cerebrospinal fluid from patients with hydrocephalus following endovascular embolization of unruptured aneurysms in comparison with other types of hydrocephalus. Neurochem Res. 2010;35:1652–8.

100. Jeppsson A, Zetterberg H, Blennow K, Wikkelso C. Idiopathic normal-pressure hydrocephalus pathophysiology and diagnosis by CSF biomarkers. Neurology. 2013;80:1385–92.

101. Pyykkö OT, Lumela M, Rummukainen J, Nerg O, Seppälä TT, Herukka S-K, et al. Cerebrospinal fluid biomarker and brain biopsy findings in idiopathic normal pressure hydrocephalus. PLoS ONE. 2014;9:e91974.

102. Alboni S, Cervia D, Sugama S, Conti B. Interleukin 18 in the CNS. J Neuroinflamm. 2010;7:9.

103. Schmitz T, Heep A, Groenendaal F, Hüseman D, Kie S, Bartmann P, et al. Interleukin-1β, interleukin-18, and interferon-γ expression in the cerebrospinal fluid of premature infants with posthemorrhagic hydrocephalus-markers of white matter damage? Pediatr Res. 2007;61:722–6.

104. Sival DA, Felderhoff-Müser U, Schmitz T, Hoving EW, Schaller C, Heep A. Neonatal high pressure hydrocephalus is associated with elevation of pro-inflammatory cytokines IL-18 and IFNγ in cerebrospinal fluid. Cerebrospinal Fluid Res. 2008;5:21.

105. Miller JM, McAllister JP. Reduction of astrogliosis and microgliosis by cerebrospinal fluid shunting in experimental hydrocephalus. Cerebrospinal Fluid Res. 2007;4:5.

106. Richards CD. The enigmatic cytokine oncostatin M and roles in disease. ISRN Inflamm. 2013;2013:512103.

107. Houben E, Hellings N, Broux B, Oncostatin M. an underestimated player in the central nervous system. Front Immunol. 2019;10:1165.

108. Gong Y, Yan X, Sun X, Chen T, Liu Y, Cao J. Oncostatin M is a prognostic biomarker and inflammatory mediator for sepsis. J Infect Dis. 2020;221:1989–98.

Lolansen *et al. Fluids and Barriers of the CNS*   (2021) 18:54

Page 15 of 15

109. West NR, Hegazy AN, Owens BMJ, Bullers SJ, Linggi B, Buonocore S, et al. Oncostatin M drives intestinal inflammation and predicts response to tumor necrosis factor–neutralizing therapy in patients with inflammatory bowel disease. Nat Med. 2017;23:579–89.

110. Cuff SM, Merola JP, Twohig JP, Eberl M, Gray WP. Toll-like receptor linked cytokine profiles in cerebrospinal fluid discriminate neurological infection from sterile inflammation. Brain Commun. 2020;2:fcaa218.

111. Wortmann A, He Y, Deryugina EI, Quigley JP, Hooper JD. The cell surface glycoprotein CDCP1 in cancer—insights, opportunities, and challenges. IUBMB Life. 2009;61:723–30.

112. Coondoo A. Cytokines in dermatology—a basic overview. Indian J Dermatol. 2011;56:368–74.

113. Marques F, Sousa JC, Coppola G, Falcao AM, Rodrigues AJ, Geschwind DH, et al. Kinetic profile of the transcriptome changes induced in the choroid plexus by peripheral inflammation. J Cereb Blood Flow Metab. 2009;29:921–32.

114. Shimada A, Hasegawa-Ishii S. Increased cytokine expression in the choroid plexus stroma and epithelium in response to endotoxin-induced systemic inflammation in mice. Toxicol Rep. 2021;8:520–8.

115. Simpson S, Preston D, Schwerk C, Schroten H, Blazer-Yost B. Cytokine and inflammatory mediator effects on TRPV4 function in choroid plexus epithelial cells. Am J Physiol Cell Physiol. 2019;317:C881–93.

116. Tarkowski E, Tullberg M, Fredman P, Wikkelsö C. Normal pressure hydrocephalus triggers intrathecal production of TNF-α. Neurobiol Aging. 2003;24:707–14.

117. Sosvorova L, Mohapl M, Vcelak J, Hill M, Vitku J, Hampl R. The Impact of selected cytokines in the follow-up of normal pressure hydrocephalus. Physiol Res. 2015;64:S283–90.

Publisher's Note